




Short Communication

# The electrical behaviors of the melilite-like solid solutions $\text{Na}_2\text{Co}(\text{P}_{2-x}\text{As}_x)\text{O}_7$ ( $x = 0.5; 1$ ): effect of the P/As substitution on structure and electrical properties

Chokri Issaoui<sup>1</sup> · Hammouda Chebbi<sup>1</sup>  · Samuel Georges<sup>2</sup> · Abderrahmen Guesmi<sup>1</sup>

Received: 11 June 2019 / Accepted: 18 October 2019 / Published online: 26 October 2019  
© Springer Nature Switzerland AG 2019

## Abstract

The melilite-like  $\text{Na}_2\text{CoP}_2\text{O}_7$  diphosphate, due to its structural features, is a promising material for sodium-ion battery cathodes. Aiming at improving the conduction properties of this phase, the  $\text{P}^{5+}$  ions were partially substituted by  $\text{As}^{5+}$  ones, and two  $\text{Na}_2\text{Co}(\text{P}_{2-x}\text{As}_x)\text{O}_7$  ( $x = 0.5$  and  $x = 1$ ) solid solutions were synthesized. The purity of the obtained solid solutions was confirmed by powder X-ray diffraction, and their electrical properties were investigated using complex impedance spectroscopy. The effects of the P/As substitution on sintering temperature, relative density and ionic conductivity were studied. The mean particle size was reduced by ball milling. The sintering temperature decreased from 680 to 640 °C from the pure phosphate to the arsenic richest solid solution, respectively, and the relative density of the pellets obtained after 120-min ball milling of the three samples showed an increase from 90 to 94%. The conductivity of the samples with the same relative density 90% was compared. The main effect of the substitution is a strong increase in the electrical conductivity, by about  $10^4$ , and a significant decrease in the activation energy. Further studies involving simulations will be carried out to correlate these observations with the structural features of the substituted phases. The obtained results may be significant for overall sodium-ion battery performance.

**Keywords**  $\text{Na}_2\text{Co}(\text{P}_{2-x}\text{As}_x)\text{O}_7$  solid solutions · X-ray diffraction · Ball milling · Structure · Ionic conductivity

## 1 Introduction

The diphosphates with the formula  $\text{A}_2\text{MP}_2\text{O}_7$  (A being an alkaline ion and M a divalent cation) are a large family of crystalline materials with many symmetries and several important physical properties [1–7]. Among these materials, the tetragonal form of the  $\text{Na}_2\text{CoP}_2\text{O}_7$  phosphate which exhibits a melilite-like structure [4, 8] was largely investigated [4, 8–11]. The studies on this form as well as its isotopic compounds show that their structures can be described as layered and formed by slabs of  $[\text{MP}_2\text{O}_7]_{\infty}^{-}$  with alkali cations located between the layers (Fig. 1a). These materials are promising since they exhibit interesting

physical properties, mainly electrical conductivity [4]. However, only few studies are devoted to the isostructural arsenates; recently, Issaoui et al. [12] reported the single-crystal structures of two  $\text{Na}_2\text{Co}(\text{P}_{2-x}\text{As}_x)\text{O}_7$  ( $x = 0.40$  and  $0.93$ ) solid solutions; their study shows that the P/As substitution induces an oxygen disorder (Fig. 1b).

Besides, if the electrical properties of many phosphate or arsenate materials have been largely investigated, only few studies were devoted to the samples densification and then the relative density and to the different parameters that can have an effect on. Indeed, it has been demonstrated in many previous studies [13–17] that the electrical behavior is closely related to the relative density, which

✉ Hammouda Chebbi, chebbamouda@yahoo.fr | <sup>1</sup>Laboratoire de Matériaux, Cristallographie et Thermodynamique Appliquée (LMCTA), Faculté des Sciences de Tunis, Université de Tunis El Manar, Manar II, 2092 Tunis, Tunisia. <sup>2</sup>Laboratoire d'Electrochimie et de Physicochimie des Matériaux et des Interfaces (LEPMI), Université Grenoble Alpes - CNRS, 1130 rue de la Piscine, 38402 Saint Martin d'Hères, France.



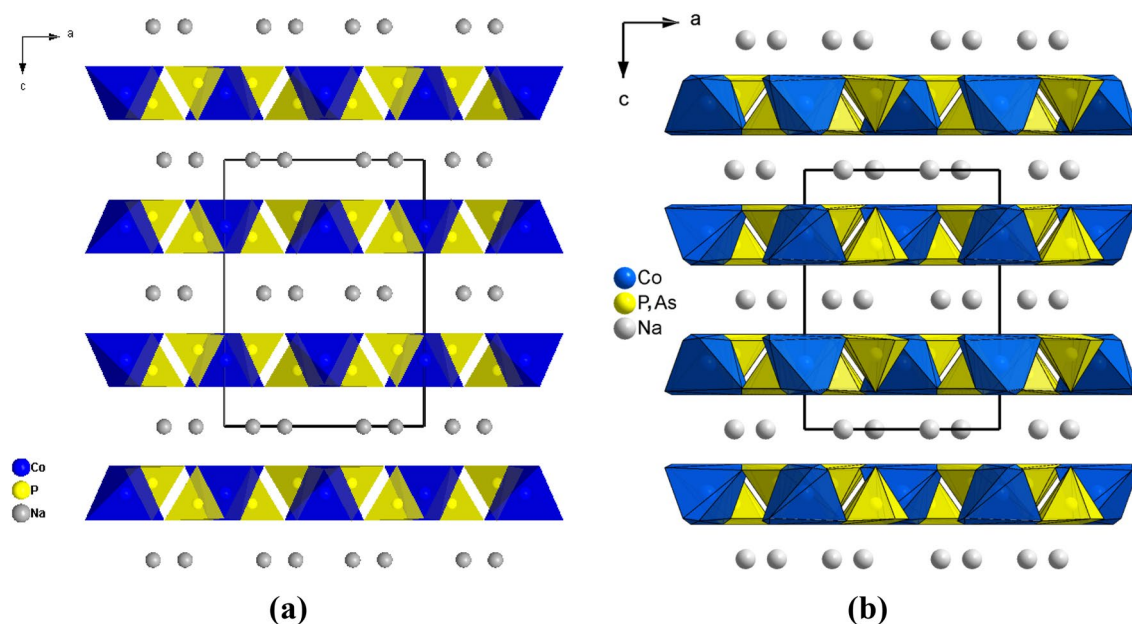


**Fig. 1** Projections along the [010] direction, showing the layer-like structures of Na<sub>2</sub>CoP<sub>2</sub>O<sub>7</sub> (a) [8] and Na<sub>2</sub>CoP<sub>1.60</sub>As<sub>0.40</sub>O<sub>7</sub> (b) [12]

points out the importance of its control. Moreover, it has been shown in many works that the best densities were obtained for arsenates rather than phosphates [14–17]. Accordingly, it is interesting to improve the relative density of phosphate materials by the substitution of P atoms by As ones. Consequently, the electrical properties could be improved.

With regard to electrical studies, ball milling was used as mechanical means to reduce the particles sizes of the synthesized Na<sub>2</sub>Co(P<sub>2-x</sub>As<sub>x</sub>)O<sub>7</sub> ( $x=0, 0.5$  and  $1$ ) powders. The electrical properties were then investigated by complex impedance spectroscopy. For comparison purposes, the electrical studies of the pure phosphate compound have been reproduced [4].

## 2 Experimental methods

### 2.1 Powder syntheses

The Na<sub>2</sub>Co(P<sub>2-x</sub>As<sub>x</sub>)O<sub>7</sub> ( $x=0, 0.5$  and  $1$ ) polycrystalline phases were obtained from mixtures of NaNO<sub>3</sub>, Co(NO<sub>3</sub>)<sub>2</sub>·6H<sub>2</sub>O, NH<sub>4</sub>H<sub>2</sub>PO<sub>4</sub> and NH<sub>4</sub>H<sub>2</sub>AsO<sub>4</sub> at Na/Co/P/As molar ratio of 2:1:(2-x):x ( $x=0, 0.5$  and  $1$ ). First, the reagents were dissolved in deionized water; the obtained solutions were evaporated to dryness at 80 °C. The solid residues were ground and then heated first at 400 °C for 24 h to eliminate the volatile products. After a second grinding, they were progressively heated at temperatures close to 600 °C and the thermal treatments were alternated by many grinding steps. Finally, the samples were

cooled down to 500 °C at 5 °C h<sup>-1</sup> and then quenched to room temperature.

### 2.2 X-ray powder diffraction

The X-ray diffraction patterns were obtained using a Bruker D8 Advance diffractometer equipped with a CuK $\alpha$  radiation ( $\lambda = 1.54056$  Å) at room temperature. The measurements were taken under Bragg–Brentano geometry at  $2\theta$  with a step of 0.017° in the range 10–70°. The cell parameters were refined using Treor program [18].

### 2.3 Electrical measurements

With regard to electrical studies, first, in order to control the microstructure and to obtain pellets with maximum relative densities, the synthesized powders were reduced by ball milling using a FRITSCH planetary micro-mill pulverisette apparatus. The milling powders were then shaped into pellets using a cylindrical steel mold by a uniaxial pressure to give the shape of a cylinder followed by isostatic pressing at 2.5 kbar. Finally, the pellets were sintered; the optimum sintering temperature for each pellet was obtained by following the relative density with the increase in temperature: The procedure followed was to heat the sample with a step of 10 °C until reaching the maximum relative density. The latter is expected at a temperature of 680 °C for Na<sub>2</sub>CoP<sub>2</sub>O<sub>7</sub> and Na<sub>2</sub>CoP<sub>1.5</sub>As<sub>0.5</sub>O<sub>7</sub> and 640 °C for Na<sub>2</sub>CoPAsO<sub>7</sub>. So, the sintering temperature was reached when the relative

density becomes constant almost at a temperature of 50 °C below the melting point of each phase. Afterward, 36-nm-thick platinum films were deposited on both faces of each sample by RF magnetron sputtering to ensure good electrical contacts with the measurement setup. Impedance spectroscopy measurements were taken using a Hewlett–Packard 4192-A spectrometer; impedance spectra were recorded at air in the 5 Hz–13 MHz frequency range with a 0.1 V alternative signal and 270–450 °C, 130–360 °C and 103–304 °C temperature ranges for  $\text{Na}_2\text{Co}(\text{P}_{2-x}\text{As}_x)\text{O}_7$  with  $x=0, 0.5$  and 1, respectively. The steps of measurements are in the order of 25–30 °C. The pellets were connected to an impedance analyzer using platinum grids and wires, then mounted in a stainless steel sample holder placed inside an alumina tube and positioned in a Pyrox furnace. A stabilization time of 30 min was systematically applied between each two successive measurements.

### 3 Results and discussion

#### 3.1 The X-ray powder diffraction

The X-ray powder diffractograms of the  $\text{Na}_2\text{Co}(\text{P}_{2-x}\text{As}_x)\text{O}_7$  ( $x=0, 0.5$  and 1) phases are shown in Fig. 2. Their similarities indicate the preservation of the tetragonal symmetry. In addition, we note that by increasing the arsenic content, the peaks are gradually shifted to lower theta angle (or high d-spacing), and this indicates an increase in the cell parameters due to the large radius of arsenic, relative to phosphorus.

The cell parameters of each phase, obtained by profile refinements, are presented in Table 1. Their variations as a function of the arsenic content are presented in Fig. 3. The cell parameters have a perfect Vegard's behavior

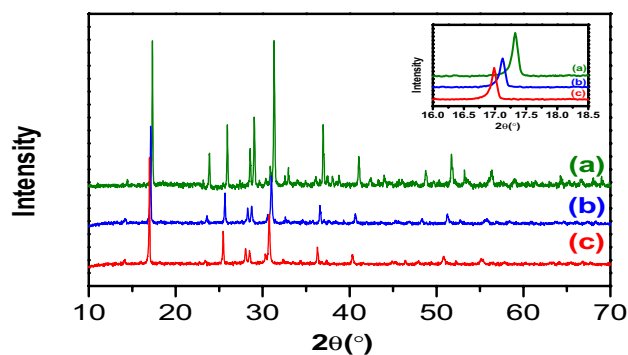


**Fig. 2** X-ray powder diffractograms of  $\text{Na}_2\text{Co}(\text{P}_{2-x}\text{As}_x)\text{O}_7$  phases. **a**  $x=0$ ; **b**  $x=0.5$ ; **c**  $x=1$

**Table 1** The refined cell parameters of the  $\text{Na}_2\text{Co}(\text{P}_{2-x}\text{As}_x)\text{O}_7$  solid solutions

Parameters	Arsenic content		
	$x=0^a$	$x=0.5$	$x=1$
$a$ (Å)	7.695 (2)	7.750 (2)	7.822 (3)
$c$ (Å)	10.280 (7)	10.347 (7)	10.447 (8)
$V$ (Å <sup>3</sup> )	608.76 (7)	621.58 (8)	639.26 (10)

<sup>a</sup>Cell parameters from Bih et al. [8]: 7.704 (3) Å; 10.296 (5) Å and Erragh et al. [11]: 7.698 (2) Å; 10.282 (2) Å

since their evolutions with an increase in arsenic content are practically linear.

#### 3.2 Electrical characterization

##### 3.2.1 Microstructure control

Prior to the electrical characterization, the sintering behavior of the powders was carefully investigated, and the ceramics microstructures controlled and optimized. Ball milling and appropriate sintering are two protocols showing good effects on relative densities of arsenates  $\text{Ag}_4\text{Co}_7(\text{AsO}_4)_6$  [16] and  $\text{Na}_4\text{Co}_7(\text{AsO}_4)_6$  [19], LAMOX materials [20, 21], etc. However, these procedures seem to be less effective for phosphate materials, as reported for  $\text{KCoP}_3\text{O}_9$  [13] and  $\text{NaCo}(\text{PO}_3)_3$  [15]. Otherwise, it has been shown in many previous works [16, 17, 20, 21] that 120-min ball milling followed by sintering temperature optimization permits to obtain a dense ceramic synthesized by solid-state reaction with small grains of about 1 μm to 50 nm [16, 17, 20, 21].

With regard to the studied phases, for each sample, two pellets were prepared from non-milled and from 120-min milled powders and the sintering temperature of each pellet has been optimized; the main results are summarized in Table 2. We notice that the ball milling allowed a gain in relative density of 3% for the phosphate and 4% for the solid solutions, and this would obviously affect the electrical properties. It can also be deduced that the P/As substitution improves sintering temperatures which decreased from 680 to 640 °C.

##### 3.2.2 Electrical properties

**3.2.2.1 The effects of ball milling and sintering** The first resolved complex impedance spectra of the three  $\text{Na}_2\text{Co}(\text{P}_{2-x}\text{As}_x)\text{O}_7$  phases ( $x=0, 0.5$  and 1) recorded at 270 °C, 185 °C and 130 °C, respectively, and with two relative densities for each phase are shown in Fig. 4. All the Nyquist diagrams are normalized by geometric factors.

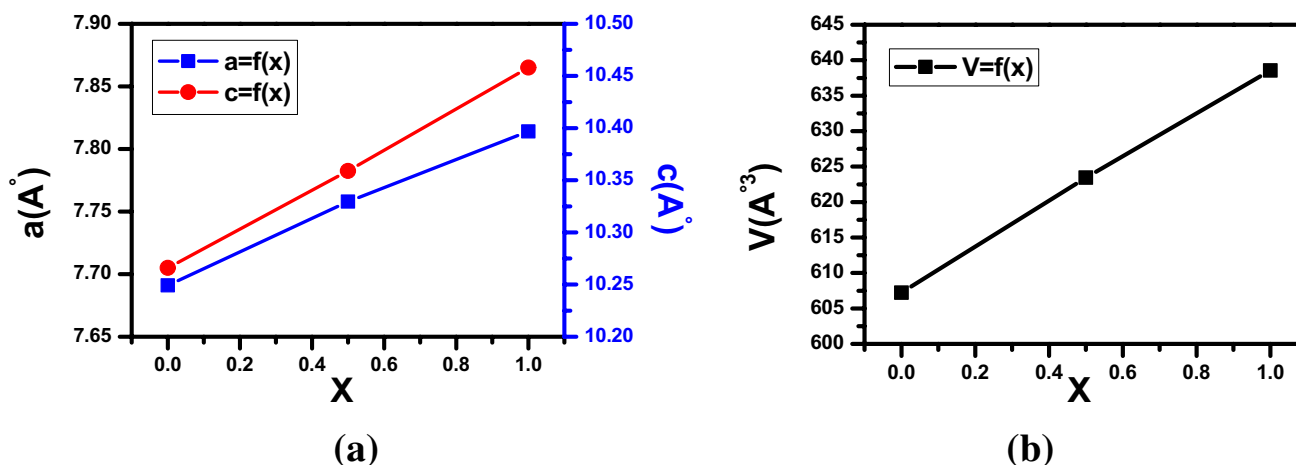


Fig. 3 Cell parameters (a) and volume (b) versus the arsenic content in the  $\text{Na}_2\text{Co}(\text{P}_{2-x}\text{As}_x)\text{O}_7$  phases

Table 2 Ceramics relative density before and after ball milling and optimized sintering temperatures

Sample	Relative density		Optimal sintering temperature (°C)
	Before milling (%)	After 120 min of milling (%)	
$\text{Na}_2\text{CoP}_2\text{O}_7$	87	90	680
$\text{Na}_2\text{CoP}_{1.5}\text{As}_{0.5}\text{O}_7$	90	94	680
$\text{Na}_2\text{CoPASO}_7$	90	94	640

Each spectrum is formed by one semicircle arc attributed to the bulk phenomena. Neither grain boundary nor polarization effects at low frequency are observed. The spectra were fitted by Zview software [22]; the equivalent circuit which provides the most realistic model of the electrical properties is formed by a resistor  $R$  connected in parallel with a constant phase element CPE, and the empirical impedance function is:

$$Z(\omega)_{\text{CPE}} = \frac{1}{Q(j\omega)^p}; \quad (-1 \leq p \leq 1)$$

where  $Q$  is the pseudo-capacity which has the numerical value of  $1/|Z|$  at  $\omega = 1$  rad/s.

The parameters  $R$ ,  $Q$  and  $p$  are obtained from the fit of the theoretical models to the experimental spectra, while the relaxation frequency  $\omega_0$ , the offset angle from the real axis  $\beta$  and the resistivity of the material  $\rho$  are calculated using the following formulas:

$$\omega_0 = (RQ)^{-1/p} = (RC)^{-1}; \quad \beta = (1-p)\frac{\pi}{2}; \quad \rho = \frac{R}{k}$$

$C$  is the real capacity of the material and  $Ck$  is the normalized capacity by the geometric factor of the pellet  $k$ .

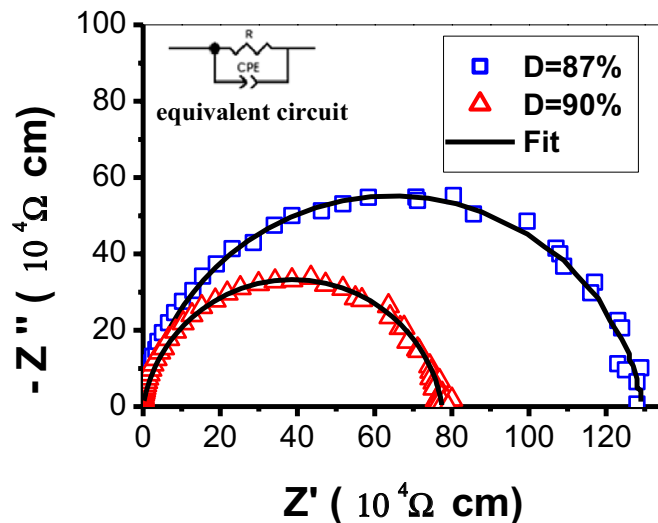
The examination of the different electrical parameters allows, according to the literature [13, 20], to deduce the following results:

- The normalized capacities ( $Ck$ ) of the different pellets are of the order of  $10^{-12}$  F cm<sup>-1</sup>, the ionic polarization relaxation is thus dominated by intra-granular effects, and the contribution of grain boundaries is absent or negligible.
- The value of the offset angle  $\beta$  with respect to the real axis is low ( $10^\circ$ ) and almost constant for all the pellets indicating a good homogeneity in the samples.
- The frequency  $\omega_0$  of each pellet increases with heating, while the capacitance ( $Ck$ ) decreases with temperature.
- A significant effect of the densification is observed. The resistivity decreases as the relative density increases, the evolution of the densities being the result of the decrease in the pore volume fraction, and consequently, the grains get closer, favoring thus the motion of  $\text{Na}^+$  cations from one grain to another. Thus, the resistive effect of the pores becomes weaker and the ceramic becomes more conductive.

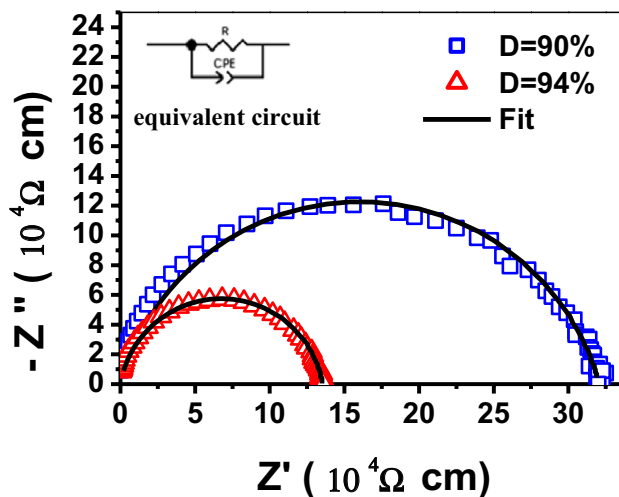
The Arrhenius diagrams presented in Fig. 5 show that the variations are linear and the effect of the microstructure, especially the porosity expressed by the relative density, is significant on the activation energy. Indeed, the relative density gain for the phosphate ceramic from 87 to 90% is manifested by the decrease in the activation energy by approximately 0.20 eV, from 0.80 to 0.60 eV. The same behavior is observed for the two solid solutions which both gained more in relative density, from 90 up to 94%, and this was manifested by the decrease in activation energy from 0.53 to 0.50 eV for  $\text{Na}_2\text{CoP}_{1.5}\text{As}_{0.5}\text{O}_7$  and from 0.51 to 0.42 eV for  $\text{Na}_2\text{CoPASO}_7$ .

**Fig. 4** Some complex impedance spectra of the three  $\text{Na}_2\text{Co}(\text{P}_{2-x}\text{As}_x)\text{O}_7$  phases

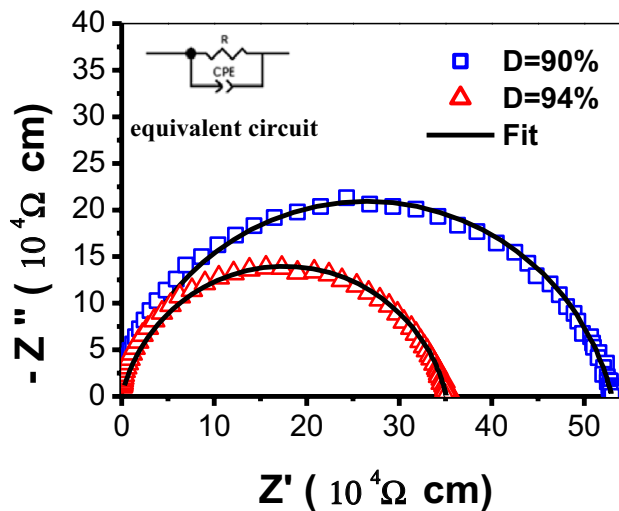
$\text{Na}_2\text{CoP}_2\text{O}_7$  at  
T=270°C



$\text{Na}_2\text{CoP}_{1.5}\text{As}_{0.5}\text{O}_7$  at  
T=185°C



$\text{Na}_2\text{CoPAsO}_7$  at  
T=130°C





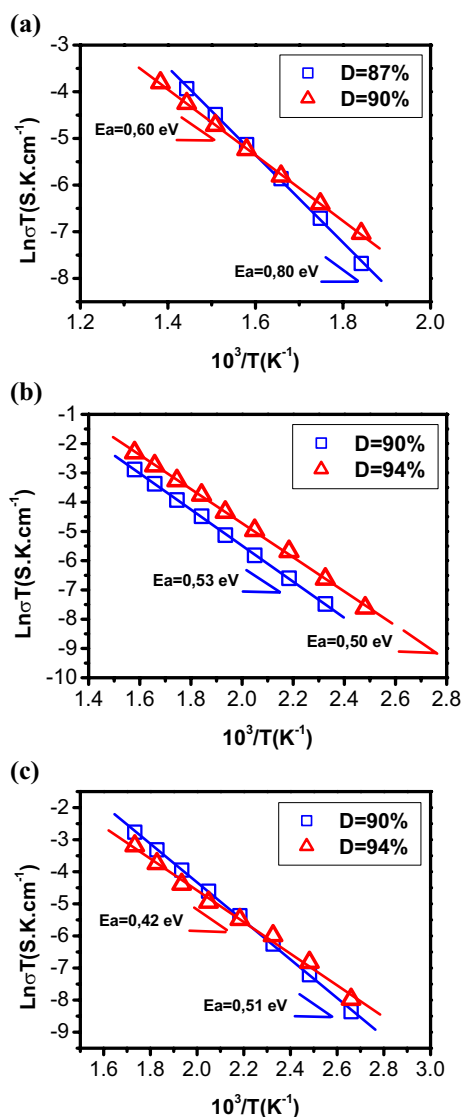


**Fig. 5** Arrhenius diagrams of the studied phases. **a**  $\text{Na}_2\text{CoP}_2\text{O}_7$ ; **b**  $\text{Na}_2\text{CoP}_{1.5}\text{As}_{0.5}\text{O}_7$ ; **c**  $\text{Na}_2\text{CoPAsO}_7$

**3.2.2.2 The effect of the P/As substitution** To find out the effect of P/As substitution on the electrical properties, three pellets with the same relative density (90%) were examined. The resulted spectra obtained at 270 °C are shown in Fig. 6. The main electrical parameters are summarized in Table 3. At these same conditions, it can be deduced that:

- The normalized capacities ( $Ck$ ) of the three pellets are about  $2 \times 10^{-12} \text{ F cm}^{-1}$ , this is consistent with ionic motion in the bulk, and therefore, the choice of the equivalent circuit is again approved.
- The frequency  $\omega_0$  increases from  $0.79 \times 10^6 \text{ rad s}^{-1}$  for  $\text{Na}_2\text{CoP}_2\text{O}_7$  to  $43.80 \times 10^6 \text{ rad s}^{-1}$  for  $\text{Na}_2\text{CoPAsO}_7$ , while

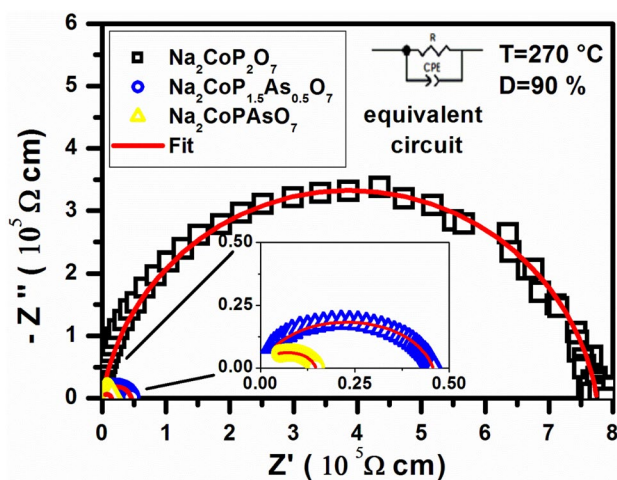


**Fig. 6** Impedance spectra recorded in air at  $\sim 270^\circ\text{C}$  on  $\text{Na}_2\text{CoP}_2\text{O}_7$ ,  $\text{Na}_2\text{CoP}_{1.5}\text{As}_{0.5}\text{O}_7$  and  $\text{Na}_2\text{CoPAsO}_7$  samples with the same relative density 90%

the capacities ( $Ck$ ) increase from  $2.04 \times 10^{-12} \text{ F cm}^{-1}$  for  $\text{Na}_2\text{CoP}_2\text{O}_7$  to  $1.52 \times 10^{-12} \text{ F cm}^{-1}$  for  $\text{Na}_2\text{CoPAsO}_7$ .

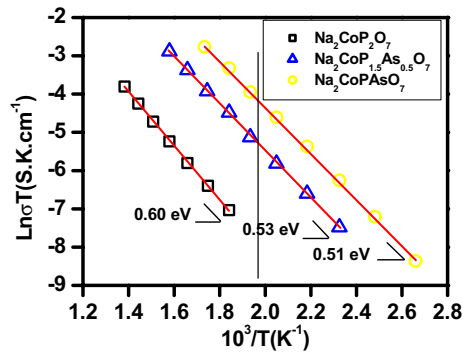
The main result of the P/As substitution is a strong increase, by about  $10^4$ , of the electrical conductivity. At the same time, the activation energy is reduced when the As fraction increases (Fig. 7). The effect of the substitution is very clear on the conductivity  $\sigma$  (Table 3) which increases at  $\sim 270^\circ\text{C}$  from  $0.16 \times 10^{-5} \text{ S cm}^{-1}$  to  $2.085 \times 10^{-5} \text{ S cm}^{-1}$  and to  $6.645 \times 10^{-5} \text{ S cm}^{-1}$  for  $\text{Na}_2\text{CoP}_2\text{O}_7$ ,  $\text{Na}_2\text{CoP}_{1.5}\text{As}_{0.5}\text{O}_7$  and  $\text{Na}_2\text{CoPAsO}_7$ , respectively, i.e., 13 times from  $\text{Na}_2\text{CoP}_2\text{O}_7$  to  $\text{Na}_2\text{CoP}_{1.5}\text{As}_{0.5}\text{O}_7$  and 41 times from  $\text{Na}_2\text{CoP}_2\text{O}_7$  to the richest As phase  $\text{Na}_2\text{CoPAsO}_7$ .

## 4 Conclusion

Two  $\text{Na}_2\text{Co}(\text{P}_{2-x}\text{As}_x)\text{O}_7$  solid solutions and the un-substituted phase were studied by XRD, and their ionic conduction properties were investigated. The partial substitution of P atoms by As ones shows several important effects: a decrease in the sintering temperature, an improvement in the relative density and a strong increase in the electrical conductivity with a decrease in the activation energy. The substitution is thus a new way to improve the electrical properties of phosphates samples; this result may then be generalized to other materials. Otherwise, we intend to complete the present work with theoretical studies in order to understand the relationships between structural modifications induced by the  $\text{As}^{5+}$  ions in the diphosphate framework and the

**Table 3** The refined electrical parameters of the equivalent circuit for the three samples with same relative density 90% at 270 °C

Sample	$R$ ( $10^3 \Omega$ )	$Q$ ( $10^{-10} \text{Fs}^{p-1}$ )	$p$	$Ck$ ( $10^{-12} \text{F cm}^{-1}$ )	$\omega_0$ ( $10^6 \text{rad s}^{-1}$ )	$\rho$ ( $10^5 \Omega \text{cm}$ )	$\beta$ ( $^\circ$ )	$\sigma$ ( $10^{-5} \text{S cm}^{-1}$ )
$\text{Na}_2\text{CoP}_2\text{O}_7$	775	6	0.90	2	0.8	62	8.7	0.16
$\text{Na}_2\text{CoP}_{1.5}\text{As}_{0.5}\text{O}_7$	46	21	0.86	2.00	10.40	4.8	12.7	2.1
$\text{Na}_2\text{CoPAsO}_7$	15	11	0.89	1.5	43.8	1.5	9.9	6.7

**Fig. 7** Arrhenius plots of conductivity of the studied samples with same relative density 90%

electrical properties improvement. This will be the subject of future works.

**Acknowledgements** Financial support from the Ministry of Higher Education, Scientific Research and Technology of Tunisia is gratefully acknowledged.

### Compliance with ethical standards

**Conflict of interest** All the authors declare that they have no conflict of interest.

### References

- El Maadi A, Boukhari A, Holt EM (1995) Crystal structures of the new diphosphates,  $\text{K}_2\text{NiP}_2\text{O}_7$  and  $\text{K}_6\text{Sr}_2\text{Ni}_5(\text{P}_2\text{O}_7)_5$ . *J Chem Crystallogr* 25:531–536
- Erragh F, Boukhari A, Abraham F, Eloudi B (1995) The crystal structure of  $\alpha$  and  $\beta$   $\text{Na}_2\text{CuP}_2\text{O}_7$ . *J Solid State Chem* 120:23–31
- Erragh F, Boukhari A, Sadel A, Holt EM (1998) Disodium zinc pyrophosphate and disodium (europium) zinc pyrophosphate. *J Acta Crystallogr C* 54:1373–1376
- Sanz F, Parada C, Rojo JM, Ruiz-Valero C, Saez-Puche R (1999) Faradaic reactions in capacitive deionization for desalination and ion separation. *J Solid State Chem* 145:604–611
- Belharouak I, Gravereau P, Parent C, Chaminade JP, Lebraud E, Le Flem G (2000) Crystal structure of  $\text{Na}_2\text{ZnP}_2\text{O}_7$ : reinvestigation. *J Solid State Chem* 152:466–473
- Dridi N, Boukhari A, Réau JM, Rbib E, Holt EM (2000) Crystal structure and ionic conductivity of crystalline and glassy  $\text{Na}_2\text{PbP}_2\text{O}_7$ . *J Solid State Ion* 127:141–149
- Dridi N, Boukhari A, Réau JM, Rbib E, Holt EM (2001) Structure and electrical properties of crystalline and glassy  $\text{Ag}_2\text{PbP}_2\text{O}_7$ . *Mater Lett* 47:212–218
- Bih H, Saadouni I, Mansori M (2006) The lamellar  $\text{Na}_2\text{CoP}_2\text{O}_7$ : preparation, structural and spectroscopic studies. *Moroc J Cond Mater* 7:74–76
- Lokanath NK, Sridhar MA, Prasad JS, Gopalakrishna GS, Ashamanjari KG (1999) Synthesis and structural characterization of  $(\text{Na}_2\text{CoP}_2\text{O}_7)_2$  crystal. *J Mater Sci Lett* 18:1723–1726
- Barpanda P, Lu J, Ye T, Kajiyama M, Chung SC, Yabuuchi N, Komaba S, Yamada A (2013) A layer-structured  $\text{Na}_2\text{CoP}_2\text{O}_7$  pyrophosphate cathode for sodium-ion batteries. *RSC Adv* 3:3857–3860
- Erragh F, Boukhari A, Elouadi B, Holt EM (1991) Crystal structures of two allotropic forms of  $\text{Na}_2\text{CoP}_2\text{O}_7$ . *J Crystallogr Spectrosc Res* 21:321–326
- Issaoui C, Chebbi H, Guesmi A (2017) The influence of P/As substitution in the melilite-like  $\text{Na}_2\text{Co}(\text{P}_{2-x}\text{As}_x)\text{O}_7$  ( $x = 0.40$  and  $0.93$ ) solid solutions. *Acta Crystallogr C* 73:331–336
- Smida YB, Guesmi A, Georges S, Zid MF (2015) Synthesis, crystal structure and electrical properties of new phosphate  $\text{KCoP}_3\text{O}_9$ . *J Solid State Chem* 221:278–284
- Smida YB, Marzouki R, Guesmi A, Georges S, Zid MF (2015) Synthesis, structural and electrical properties of a new cobalt arsenate  $\text{NaCo}_2\text{As}_3\text{O}_{10}$ . *J Solid State Chem* 221:132–139
- Smida YB, Guesmi A, Georges S, Avdeev M, Zid MF (2016) Crystal structure and ionic conductivity of the new cobalt polyphosphate  $\text{NaCo}(\text{PO}_3)_3$ . *J Solid State Chem* 234:15–21
- Marzouki R, Guesmi A, Georges S, Zid MF, Driss A (2014) Structure, sintering and electrical properties of new ionic conductor  $\text{Ag}_4\text{Co}_7(\text{AsO}_4)_6$ . *J Alloy Compd* 586:74–79
- Marzouki R, Guesmi A, Zid MF, Driss A (2013) Electrical properties and  $\text{Na}^+$  mobility in  $\text{Na}_4\text{Co}_{5.63}\text{Al}_{0.91}(\text{AsO}_4)_6$  material. *J Inorg Chem* 1:9–16
- Werner PE, Eriksson L, Westdahl M (1985) TREOR, a semi-exhaustive trial-and-error powder indexing program for all symmetries. *J Appl Crystallogr* 18:367–370
- Smida YB, Marzouki R, Georges S, Kutteh R, Avdeev M, Guesmi A, Zid MF (2016) Synthesis, crystal structure, electrical properties, and sodium transport pathways of the new arsenate  $\text{Na}_4\text{Co}_7(\text{AsO}_4)_6$ . *J Solid State Chem* 239:8–16
- Georges S, Goutenoire F, Lacorre P, Steil MC (2005) Sintering and electrical conductivity in fast oxide ion conductors  $\text{La}^{2-x}\text{R}_x\text{Mo}^{2-y}\text{W}_y\text{O}_9$  (R: Nd, Gd, Y). *J Eur Ceram Soc* 25:3619–3627
- Georges S, Goutenoire F, Altorf F, Sheptyakov D, Fauth F, Suard E, Lacorre P (2003) Thermal, structural and transport properties of the fast oxide-ion conductors  $\text{La}^{2-x}\text{R}_x\text{Mo}_2\text{O}_9$  (R= Nd, Gd, Y). *Solid State Ion* 161:231–241
- Johnson D (1990–2007) Zview version 3.1c. Scribner Associates Inc., Southern Pines

**Publisher's Note** Springer Nature remains neutral with regard to jurisdictional claims in published maps and institutional affiliations.